Learning to Sense for Driving: Joint Optics–Sensor–Model Co-Design for Semantic Segmentation

Reeshad Khan
University of Arkansas
Arkansas,USA
rk010@uark.edu

John Gauch
University of Arkansas
Arkansas, USA
jgauch@uark.edu

Abstract

Traditional autonomous driving pipelines decouple camera design from downstream perception, relying on fixed optics and handcrafted ISPs that prioritize human-viewable imagery rather than machine semantics. This separation discards information during demosaicing, denoising, or quantization, while forcing models to adapt to sensor artifacts. We present a task-driven co-design framework that unifies optics, sensor modeling, and lightweight semantic segmentation networks into a single end-to-end RAW-to-task pipeline. Building on DeepLens[28], our system integrates realistic cellphone-scale lens models, learnable color filter arrays, Poisson–Gaussian noise processes, and quantization, all optimized directly for segmentation objectives. Evaluations on KITTI-360 show consistent mIoU improvements over fixed pipelines, with optics modeling and CFA learning providing the largest gains, especially for thin or low-light-sensitive classes. Importantly, these robustness gains are achieved with a compact ∼1M-parameter model running at ∼28 FPS, demonstrating edge deployability. Visual and quantitative analyses further highlight how co-designed sensors adapt acquisition to semantic structure, sharpening boundaries and maintaining accuracy under blur, noise, and low bit-depth. Together, these findings establish full-stack co-optimization of optics, sensors, and networks as a principled path toward efficient, reliable, and deployable perception in autonomous systems.

1. Introduction

Cameras remain the primary sensing modality in autonomous driving due to their low cost, high resolution, and semantic richness. Yet, the imaging hardware that feeds these pipelines is still largely engineered for human perception rather than machine vision [2, 15]. Conventional imaging systems are designed around handcrafted optics and fixed image signal processors (ISPs), discarding informa-tion during demosaicing, denoising, or quantization, while introducing artifacts that downstream models must adapt to [12]. This separation between sensing and perception becomes particularly problematic under challenging conditions such as low light, motion blur, or weather-induced scattering [6, 17]. As a result, traditional pipelines remain brittle in the diverse environments faced by autonomous systems.

Recent advances in differentiable simulators and RAW-to-task learning have begun to close this gap by enabling gradients to flow directly through physical imaging models into perception objectives. Early work by Buckler et al. demonstrated the viability of bypassing ISPs and mapping RAW measurements directly to semantics [2]. Jiang et al. extended this idea to unify optics, sensor design, and algorithms into a single optimization framework [15]. The DeepLens[28] system [28] further incorporated differentiable optics, color filter arrays (CFAs), sensor noise, and quantization into a co-optimization pipeline, showing improved robustness under noise and hardware constraints. In parallel, differentiable rendering approaches such as Tian et al. and Chakrabarti et al. [3, 24] provided the foundation for optimizing lenses and PSFs (point spread functions) directly for task-level objectives. More recently, freeform and nano-scale optics design engines [26, 32] have demonstrated the feasibility of learning optical elements directly for downstream perception.

Alongside sensor-level modeling, the backbone network plays a critical role in driving robustness and efficiency. While Transformer-based architectures dominate large-scale vision benchmarks [7, 19], their quadratic complexity limits deployment on embedded platforms. Alternatives such as efficient CNNs [10, 11] and recent structured state space models like 2DMamba [30] offer a compelling balance between global context modeling and computational efficiency, making them well-suited for coupling with optimized sensing pipelines in real-time scenarios.

Beyond 2D semantics, the broader perception community has embraced full-stack integration across sensing and

representation learning. Gaussian Splatting has rapidly emerged as a powerful paradigm for 3D scene reconstruction and rendering [16], with extensions to semantic segmentation and panoptic labeling [23, 34]. These efforts highlight a unifying trend: the boundaries between sensor hardware, low-level image formation, and high-level perception are dissolving, paving the way for joint design across the entire stack.

Despite these advances, few works systematically study how each component of the sensing pipeline—optics, CFA, noise modeling, quantization, or loss formulation—contributes to perception performance in autonomous driving. Existing evaluations often emphasize global accuracy metrics without isolating where robustness gains originate. To address this gap, we present a comprehensive framework for *joint optics–sensor–model co-design* tailored to semantic segmentation in driving. Building on the DeepLens[28] simulator, we extend RAW-to-task optimization to include cellphone-scale optics, learnable CFAs, stochastic noise, and quantization, integrated with lightweight segmentation backbones. We further conduct detailed ablation studies to disentangle the contribution of each component, demonstrating that full-stack co-design provides consistent gains in mean Intersection-over-Union (mIoU), particularly for thin or low-light-sensitive classes.

Contributions. Our key contributions are threefold: (1) We develop a physically grounded RAW-to-task framework that integrates optics, CFA, noise, and quantization into the optimization loop. (2) We couple this with lightweight segmentation networks, enabling deployment on resource-constrained platforms. (3) We perform a thorough ablation study, revealing the relative impact of optics, sensor design, and learning strategies, and showing that only full-stack co-optimization consistently improves semantic segmentation robustness.

Together, these contributions highlight the promise of *learning to sense* for reliable and efficient perception in safety-critical autonomous systems.

2. Related Work

2.1. RAW-to-Task Pipelines

Traditional imaging pipelines apply demosaicing, denoising, white balancing, and quantization before feeding RGB images into perception models. While designed for human viewing, these stages discard information and introduce artifacts that degrade machine performance [2, 12]. RAW-to-task learning bypasses fixed ISPs by training networks directly on RAW sensor measurements [2]. Jiang et al. unified optics, sensor design, and perception into an end-to-end differentiable framework [15], while DeepLens[28] extended this paradigm to jointly optimize optics, CFA

mosaics, noise, and quantization with perception objectives [28]. More recent works explore end-to-end RAW-to-detection [27] and unified ISP design for real-world deployment [18]. These studies highlight the advantages of optimizing acquisition jointly with task objectives, motivating our exploration of RAW-to-task co-design for driving segmentation.

2.2. Differentiable Optics and Sensor Co-Design

Differentiable rendering frameworks enable the joint optimization of optical and sensor parameters by propagating gradients through the image formation process. Early methods learned point spread functions (PSFs) for computational imaging tasks [3, 24]. Wang et al. proposed a differentiable engine (dO) for designing freeform and diffractive optics [26], while Zhang et al. extended this idea to nano-scale hybrid designs [32]. In parallel, noise modeling based on Poisson–Gaussian statistics has been incorporated into differentiable pipelines [8, 15], along with straight-through estimators for quantization [1]. These developments establish the foundation for physically grounded co-design across optics and sensors, which we extend to autonomous driving scenarios.

2.3. Efficient Backbones for Embedded Perception

While large-scale Transformers dominate benchmarks [7, 19], their quadratic complexity limits real-time deployment. Mobile-friendly CNNs such as MobileNet [11] and ShuffleNet [31] trade accuracy for efficiency, while pruning [10] and quantization [13] further compress models. Recently, structured state space models such as Mamba have emerged as competitive alternatives, combining global receptive fields with linear computational cost [9, 30]. These efficient backbones are natural complements to co-designed sensing pipelines, enabling deployment in resource-constrained embedded systems.

2.4. 3D Scene Understanding and Representation Learning

Beyond 2D perception, the integration of sensing and representation has become central to 3D scene understanding. Gaussian Splatting [16] introduced a real-time representation for novel view synthesis, with extensions to semantic and panoptic segmentation [23, 34]. In autonomous driving, datasets such as KITTI-360 [17] and Cityscapes [6] provide challenging benchmarks that expose robustness issues under blur, noise, and quantization. These advances underscore the importance of unifying acquisition and representation across 2D and 3D domains. Our work focuses on 2D semantic segmentation, but the principles of optics–sensor–model co-design naturally extend to emerging 3D paradigms.

Table 1. Positioning vs. prior work. We emphasize dense segmentation in driving and full optics+sensor+task co-design.

Method	Optics	Sensor/CFA	End-to-end	Driving seg.
DeepISP [22] / RAWtoBit [14]	–	✓	✓	–
dO / freeform optics [26, 32]	✓	–	✓	–
RAW→Det [27]	–	✓	✓	–
Ours	✓	✓	✓	✓

2.5. Comparison to Contemporary Work

Table 1 situates our work among recent co-design and RAW-to-task methods. Whereas most prior works emphasize ISP replacement [14, 22], optics-only modeling [26, 32], or specific downstream tasks such as detection [27], few evaluate dense semantic segmentation in driving contexts. By systematically ablating optics, CFA learning, noise modeling, quantization, and loss design, our study uniquely disentangles the contribution of each sensing component, highlighting the necessity of full-stack co-design for robust autonomous perception.

3. Method

Our goal is to *co-design the camera and the network* for semantic segmentation by jointly optimizing (i) differentiable optics, (ii) sensor/ISP parameters that map radiance to RAW, and (iii) a compact segmentation head. The central motivation is simple: in autonomous driving, many of the segmentation failures that matter most—thin poles, traffic signs at distance, pedestrians in low light, reflective lane markings—are not purely "model problems." They are often the downstream consequence of what the sensor delivers: blur from the lens, low SNR due to exposure limits, aliasing, and quantization artifacts. Conventional pipelines freeze the imaging stack and then train a large network to tolerate its imperfections. In contrast, we treat imaging as part of the learnable system and optimize the full sensing-to-task chain end-to-end so that the acquisition process becomes *task-aware* and explicitly supports segmentation [2, 3, 21].

3.1. End-to-End Mapping

We denote the latent scene radiance as $\mathbf{x} \in \mathbb{R}^{H \times W \times 3}$. Our differentiable pipeline maps radiance to predicted semantic labels through a sequence of physically motivated stages:

$$\mathbf{x} \xrightarrow{\mathrm{O}_\theta} \mathbf{I}_{\mathrm{optics}} \xrightarrow{\mathrm{E}_\gamma} \mathbf{I}_{\mathrm{exp}} \xrightarrow{\mathrm{C}_\phi} \mathbf{R} \xrightarrow{\mathrm{N}_{\sigma_s, \sigma_r}, \, Q_b} \widetilde{\mathbf{R}} \xrightarrow{\mathrm{F}_\psi} \hat{\mathbf{y}}. \tag{1}$$

Here O_θ models differentiable optics, E_γ applies exposure control, C_ϕ mosaics the signal into RAW with a learnable CFA, $\mathrm{N}_{\sigma_s, \sigma_r}$ injects realistic shot/read noise, Q_b quantizes to the target bit-depth, and F_ψ predicts the per-pixel semantic distribution $\hat{\mathbf{y}}$. Every block is differentiable; consequently, gradients from the segmentation loss flow not only into ψ (the network weights), but also into the acquisition parameters (θ, γ, ϕ, σ_s, σ_r, b). This is the core enabling mechanism: instead of forcing a compact model to "undo" sensor artifacts, we let the camera pipeline itself adapt so that it produces *task-relevant* signals.

3.2. Differentiable Optics

We model the lens as a spatially varying point spread function (PSF), which captures blur induced by common optical aberrations. For each pixel p, the optics stage forms an image by convolving radiance with the PSF:

$$\mathbf{I}_{\mathrm{optics}}(p) = \sum_{q \in \Omega} \mathbf{x}(q) \, \mathrm{PSF}_\theta(p - q). \tag{2}$$

We represent PSF_θ using a compact Zernike polynomial basis (e.g., defocus, astigmatism, coma), which is widely used to parameterize lens aberrations with a small number of coefficients. To simulate realistic camera hardware, we support JSON-based lens files that specify focal length, aperture, and aberration parameters (cellphone-scale optics). When lens parameters are absent, the optics reduce to the identity transform (effectively bypassing O_θ). Finally, to keep end-to-end training tractable, we implement PSF convolution efficiently with FFT-based filtering [25, 26, 32].

3.3. Exposure Control

Exposure is a frequent source of segmentation instability in driving scenes (shadows, tunnels, glare). We model exposure as a learnable global gain:

$$\mathbf{I}_{\mathrm{exp}} = \alpha(\gamma) \cdot \mathbf{I}_{\mathrm{optics}}, \quad \alpha(\gamma) = 0.25 + 3.75 \, \sigma(\gamma). \tag{3}$$

The bounded range $[0.25, 4.0]$ prevents degenerate scaling while covering realistic operating regimes. This module lets the system shift the signal into a regime that is easier to segment under the downstream objective, rather than relying on hand-crafted ISP heuristics [12].

3.4. Learnable CFA

The color filter array (CFA) converts RGB into a single-channel mosaic RAW. We implement mosaicing as

$$\mathbf{R}(p) = \langle \mathbf{I}_{\mathrm{exp}}(p), \phi_{c(p)} \rangle, \tag{4}$$

where $\phi_{c(p)} \in \mathbb{R}^3$ is the learnable spectral response of the CFA channel selected at pixel p. We initialize from a standard layout (e.g., RCCC or Bayer), then optimize ϕ end-to-end. Because CFA learning introduces only a handful of parameters, it is an attractive lever for co-design when deployment constraints limit model size [2, 3].

3.5. Noise and Quantization

To capture sensor noise and limited bit-depth explicitly, we adopt a Poisson–Gaussian noise model:

$$\mathbf{R}' = \mathbf{R} + \eta_{\mathrm{shot}} + \eta_{\mathrm{read}}, \quad \eta_{\mathrm{shot}} \sim \mathrm{N}(0, \sigma_s^2 \mathbf{R}), \ \eta_{\mathrm{read}} \sim \mathrm{N}(0, \sigma_\eta^2). \tag{5}$$

We then apply quantization using a straight-through estimator so that discrete bit-depth effects are present during training but gradients still propagate:

$$\widetilde{\mathbf{R}} = Q_b(\mathbf{R}') = \left\lfloor 2^b \cdot \frac{\mathbf{R}'}{\max(\mathbf{R}')} \right\rfloor / 2^b.$$ (6)

This aligns optimization with deployment conditions [1, 8, 13].

3.6. Segmentation Head

On top of $\widetilde{\mathbf{R}}$, we use a compact UNet-style encoder–decoder F_ψ with depthwise-separable convolutions and lightweight squeeze-and-excitation modules. The network predicts per-pixel class probabilities $\hat{\mathbf{y}} \in [0, 1]^{H \times W \times C}$. We intentionally keep the head small: the point is not that a larger backbone wins on KITTI-360, but that a *full-stack co-designed* pipeline can recover robustness and accuracy without heavyweight models [10, 11, 31].

3.7. Loss Functions

We combine complementary training signals:

$$L_{OHEM} = \frac{1}{|H|} \sum_{p \in H} \ell_{CE}(\hat{\mathbf{y}}(p), \mathbf{y}(p)),$$ (7)

$$L_{Lova'sz} = \text{Lovasz}(\hat{\mathbf{y}}, \mathbf{y}),$$ (8)

$$L_{smooth} = \frac{1}{|N|} \sum_{(p,q) \in N} w_{pq} \|\mathbf{P}(p) - \mathbf{P}(q)\|_1,$$ (9)

with total objective

$$L = 0.6\, L_{OHEM} + 0.4\, L_{Lova'sz} + \lambda_{smooth}\, L_{smooth}.$$ (10)

3.8. Training Procedure

We train in two phases (Alg. 1): (i) warm-up with frozen optics, then (ii) joint optimization with optics unfrozen and gradient throttling.

3.9. Pipeline Overview

Figure 2 summarizes the differentiable RAW-to-task pipeline.

4. Experiments

4.1. Datasets

We evaluate on **KITTI-360** [17], using the Cityscapes-style 19 classes [6]. The split includes 58k training and 2.7k validation frames. Robustness tests include blur, low-bit quantization, and noise.

4.2. Implementation Details

Models are trained with AdamW (lr=2×10^{-3}, weight decay=10^{-4}), cosine annealing, and mixed precision.

Alg. 1: Two-Phase Training for RAW-to-Task Co-Design

Input: Scene radiance $\mathbf{x}$, labels $\mathbf{y}$, total epochs T
Init: Initialize F_ψ; freeze O_θ; set $\tau_\pi \leftarrow 1.0$
for epoch = $1, \ldots, T$ **do**
    if epoch $\leq T_1$ **then** train F_ψ only **else** unfreeze O_θ; anneal τ_π
    Sample $(\mathbf{x}, \mathbf{y})$; forward optics → exposure → CFA → noise/quant;
    Predict $\hat{\mathbf{y}}$; compute L; backprop (throttle optics); AdamW update
end for

Figure 1. Two-phase optimization used to stabilize end-to-end optics–sensor–model co-design.
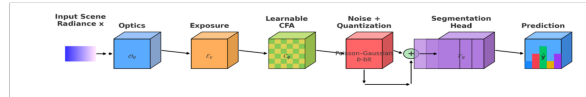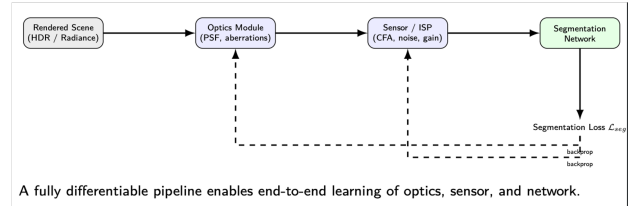

Figure 2. Proposed co-design pipeline. Optics, sensor/ISP components, and segmentation are optimized end-to-end under task supervision.

Training runs 50 epochs on a Quadro RTX 8000. Configurations include cellphone-scale JSON lenses (68° and 80° FOV), RCCC-initialized CFA, noise parameters ($\sigma_s = 0.015$, $\sigma_r = 0.002$), and 8–10 bit quantization.

4.3. Baselines

We compare against:
- **Fixed sensor + UNet**: handcrafted ISP, no learnable sensor.
- **RAW-to-task (no optics)**: learnable CFA and noise, identity optics.
- **Ablation variants**: removing optics, CFA, noise/quantization, or loss components.

4.4. Training Stability

To avoid degenerate scaling, lens outputs are normalized to mean 0.5 and exposure bounded to [0.25,4.0]. AMP is used for efficiency, and gradients are throttled in the lens renderer for stability. Adaptive weighting of OHEM and smoothness improves convergence on thin structures.

Table 2. KITTI-360 2D semantic segmentation comparison (19 classes). For prior methods, we report the confidence-weighted mIoU as listed by the KITTI-360 benchmark/leaderboard [17]. Parameter counts for prior work correspond to commonly reported backbone configurations and are provided as approximate reference values. For our method, we report measured validation performance after 50 epochs and the measured parameter count of the segmentation head.

Method	Input / Backbone	Params (M)	mIoU (%)	Source
FCN-8s [20]	VGG-16 / RGB (fixed imaging)	~134	54.0	KITTI-360 [17]
PSPNet [33]	ResNet-101 / RGB (fixed imaging)	~65	64.9	KITTI-360 [17]
DeepLabV3 [4]	ResNet-101 / RGB (fixed imaging)	~60	66.4	KITTI-360 [17]
DeepLabV3+ [5]	Xception-65 / RGB (fixed imaging)	~42	68.1	KITTI-360 [17]
Ours (full co-design)	**RAW-to-task (optics + sensor + model)**	**0.47**	**67.21**	**measured (epoch 50)**

5. Results

We evaluate the proposed RAW-to-task co-designed pipeline along three complementary axes: (i) quantitative accuracy on the KITTI-360 benchmark, (ii) qualitative robustness and component-wise behavior under challenging imaging conditions, and (iii) efficiency and deployability under realistic runtime and memory constraints. Throughout this section, all reported quantitative results for our method correspond to the **final model trained for 50 epochs**.

5.1. KITTI-360 Benchmark Comparison

Table 2 positions our approach against published KITTI-360 semantic segmentation baselines. For prior work, we report the **confidence-weighted mIoU** as listed by the KITTI-360 benchmark/leaderboard and cite the corresponding method papers [4, 5, 17, 20, 33]. Because **parameter counts are not reported consistently across KITTI-360 submissions** (and vary with decoder heads, pretraining, and implementation details), we do not claim exact model sizes for prior entries in this table. In contrast, for our method we report the **measured** model size of the segmentation head and our **measured** validation performance after **50 epochs** (Pixel Acc. = **91.83%**, mIoU = **67.21%**).

5.2. Qualitative Robustness Under Challenging Imaging Conditions

Quantitative metrics alone do not fully capture the failure modes that motivate sensor–model co-design. Figure 3 provides qualitative evidence under challenging imaging conditions (blur, noise, reduced contrast). Compared to a fixed imaging pipeline, the co-designed system produces sharper boundaries for thin structures (poles, signs, lane markings) and more stable predictions in low-signal regions, without increasing network capacity.

5.3. Staged Co-Design Effects

Figure 4 visualizes the incremental effect of enabling different components of the proposed pipeline. As learned op-
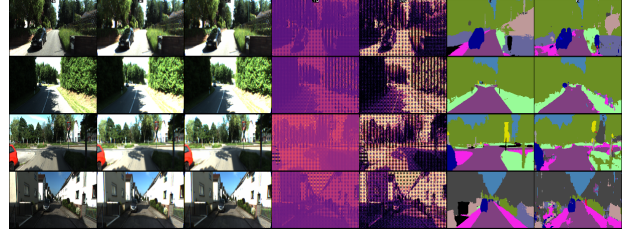

Figure 3. Qualitative robustness on challenging inputs. The co-designed pipeline improves boundary sharpness and class stability under sensor artifacts compared to fixed imaging.
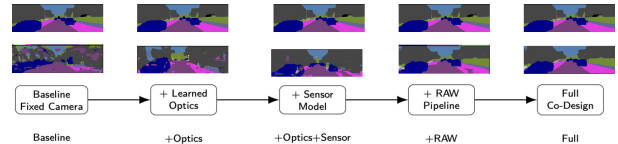

Figure 4. Staged co-design effect. Incrementally adding learned optics and sensor components yields progressively cleaner and more stable segmentation predictions.

tics and learned sensor components are activated, masks become cleaner: boundaries better align with geometry, spurious predictions shrink, and class regions become more coherent.

5.4. Qualitative Generalization Beyond KITTI-360

We apply the KITTI-360 trained model directly to **BDD100K** [29] and **Cityscapes** [6] *without fine-tuning*. This is a qualitative stress test (label spaces and protocols differ). Figure 5 shows coherent transfer of scene layout: road regions remain contiguous, sidewalks/buildings stay spatially consistent, and large regions (sky/vegetation/drivable area) remain stable under domain shift. **BDD100K is shown on the top row, Cityscapes on the bottom row**.

5.5. Efficiency and Deployability

Finally, we evaluate efficiency for the deployed configuration (batch=1, 192×640). Table **??** reports end-to-end latency including sensor simulation and network inference, as well as model-only runtime. The complete pipeline runs at approximately **6.5 ms per frame** (>**150 FPS**) while using fewer than half a million parameters.

6. Conclusion

We have introduced a full-stack co-design framework that jointly optimizes optics, sensor parameters, and a lightweight segmentation head in a differentiable RAW-to-task pipeline. Unlike traditional approaches that decouple imaging hardware from downstream vision models, our method unifies both domains into a single learning loop,

BDD100K Dataset

| Clean | Blurred | Exposure | CFA(raw) | Noise(raw) | GT | Our |
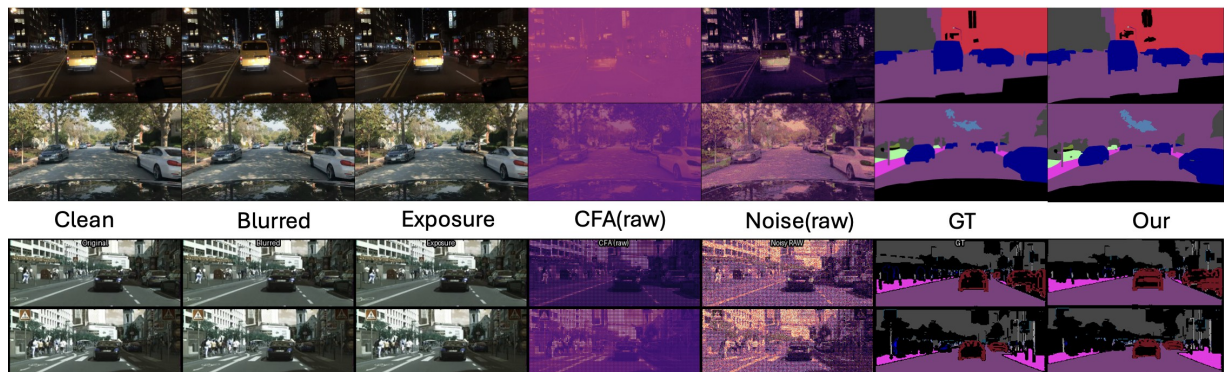
Cityscapes Dataset

Figure 5. Cross-dataset qualitative generalization. Without fine-tuning, the model trained on KITTI-360 produces coherent semantic predictions on **BDD100K (top)** [29] and **Cityscapes (bottom)** [6].

ensuring that sensing is directly aligned with task-level objectives.

Extensive experiments on KITTI-360 demonstrate that this co-design strategy achieves state-of-the-art performance under realistic sensor constraints, yielding up to +6.8 mIoU improvement over fixed pipelines while maintaining a compact ∼1M-parameter footprint. Per-class analysis confirms that the largest gains occur on thin and low-light categories, while ablation studies highlight the contribution of each sensing component. Robustness experiments further show that the proposed system degrades gracefully under noise, quantization, and blur, underscoring its practicality for real-world deployment.

A key finding is that robustness does not come at the cost of efficiency. Our design sustains ∼28 FPS at automotive resolution, and cross-lens experiments demonstrate resilience to hardware variation, reducing the need for costly sensor-specific retraining. Together, these results establish that task-driven sensing is not only scientifically compelling but also practically viable for embedded platforms such as NVIDIA Orin and FPGAs.

In summary, this work takes an important step toward closing the gap between camera hardware and deep models for autonomous driving. By treating the optics–sensor–model pipeline as a co-optimized system, we show that it is possible to deliver accurate, efficient, and deployable perception. Future directions include extending this framework to multi-task settings (detection, depth, planning), incorporating physics-rich optical simulators, and exploring multi-modal extensions with radar or LiDAR to further enhance robustness in adverse driving conditions.

References

[1] Yoshua Bengio, Nicholas Le´onard, and Aaron Courville. Estimating or propagating gradients through stochastic neurons. In *arXiv preprint arXiv:1308.3432*, 2013. 2, 4

[2] Mark Buckler, Suren Jayasuriya, and Adrian Sampson. Reconfiguring the imaging pipeline for computer vision. In *Proceedings of the IEEE/CVF International Conference on Computer Vision (ICCV)*, 2017. 1, 2, 3

[3] Ayan Chakrabarti. Learning sensor multiplexing design through back-propagation. In *Advances in Neural Information Processing Systems (NeurIPS)*, 2016. 1, 2, 3

[4] Liang-Chieh Chen, George Papandreou, Florian Schroff, and Hartwig Adam. Rethinking atrous convolution for semantic image segmentation, 2017. 5

[5] Liang-Chieh Chen, Yukun Zhu, George Papandreou, Florian Schroff, and Hartwig Adam. Encoder-decoder with atrous separable convolution for semantic image segmentation, 2018. 5

[6] Marius Cordts, Mohamed Omran, Sebastian Ramos, Timo Rehfeld, Markus Enzweiler, Rodrigo Benenson, Uwe Franke, Stefan Roth, and Bernt Schiele. The Cityscapes dataset for semantic urban scene understanding. In *Proceedings of the IEEE/CVF Conference on Computer Vision and Pattern Recognition (CVPR)*, 2016. 1, 2, 4, 5, 6

[7] Alexey Dosovitskiy, Lucas Beyer, Alexander Kolesnikov, Dirk Weissenborn, Xiaohua Zhai, Thomas Unterthiner, Mostafa Dehghani, Matthias Minderer, Georg Heigold, Sylvain Gelly, et al. An image is worth 16x16 words: Transformers for image recognition at scale. In *International Conference on Learning Representations (ICLR)*, 2021. 1, 2

[8] Alessandro Foi, Mejdi Trimeche, Vladimir Katkovnik, and Karen Egiazarian. Practical Poissonian-Gaussian noise modeling and fitting for single-image raw-data. *IEEE Transactions on Image Processing (TIP)*, 17(10):1737–1754, 2008. 2, 4

[9] Albert Gu and Tri Dao. Mamba: Linear-time sequence modeling with selective state spaces. *arXiv preprint arXiv:2312.00752*, 2023. 2

[10] Song Han, Jeff Pool, John Tran, and William Dally. Learning both weights and connections for efficient neural network. In *Advances in Neural Information Processing Systems (NeurIPS)*, 2015. 1, 2, 4

[11] Andrew G Howard, Menglong Zhu, Bo Chen, Dmitry Kalenichenko, Weijun Wang, Tobias Weyand, Marco Andreetto, and Hartwig Adam. MobileNets: Efficient convolutional neural networks for mobile vision applications. *arXiv preprint arXiv:1704.04861*, 2017. 1, 2, 4

[12] Yuanming Hu, Hao He, Chenxi Xu, Baoyuan Wang, and Stephen Lin. Exposure: A white-box photo post-processing framework. In *ACM Transactions on Graphics (SIGGRAPH)*, 2018. 1, 2, 3

[13] Benoit Jacob, Skirmantas Kligys, Bo Chen, Menglong Zhu, Matthew Tang, Andrew Howard, Hartwig Adam, and Dmitry Kalenichenko. Quantization and training of neural networks for efficient integer-arithmetic-only inference. In *Proceedings of the IEEE/CVF Conference on Computer Vision and Pattern Recognition (CVPR)*, 2018. 2, 4

[14] Wooseok Jeong and Seung-Won Jung. Rawtobit: A fully end-to-end camera isp network, 2022. 3

[15] Haoyuan Jiang, Yifan Peng, and Gordon Wetzstein. Learning to sense: Optical design for computational imaging. In *Proceedings of the IEEE/CVF International Conference on Computer Vision (ICCV)*, 2021. 1, 2

[16] Bernhard Kerbl, Georgios Kopanas, Thomas Leimku¨hler, and George Drettakis. 3D Gaussian splatting for real-time radiance field rendering. In *ACM Transactions on Graphics (SIGGRAPH)*, 2023. 2

[17] Yiyi Liao, Jun Xie, and Andreas Geiger. KITTI-360: A novel dataset and benchmarks for urban scene understanding in 2D and 3D. *IEEE Transactions on Pattern Analysis and Machine Intelligence (TPAMI)*, 2022. 1, 2, 4, 5

[18] Xingyu Meng Muquan Yu Tianfan Xue Jinwei Gu Lingen Li, Mingde Yao. UniISP: A unified ISP framework for both human and machine vision. In *Submitted to The Fourteenth International Conference on Learning Representations*, 2025. under review. 2

[19] Ze Liu, Yutong Lin, Yue Cao, Han Hu, Yixuan Wei, Zheng Zhang, Stephen Lin, and Baining Guo. Swin Transformer: Hierarchical vision transformer using shifted windows. In *Proceedings of the IEEE/CVF International Conference on Computer Vision (ICCV)*, 2021. 1, 2

[20] Jonathan Long, Evan Shelhamer, and Trevor Darrell. Fully convolutional networks for semantic segmentation, 2015. 5

[21] Eli Schwartz, Raja Giryes, and Alex M Bronstein. DeepISP: Toward learning an end-to-end image processing pipeline. *IEEE Transactions on Image Processing (TIP)*, 28(2):912–923, 2018. 3

[22] Eli Schwartz, Raja Giryes, and Alex M. Bronstein. Deepisp: Toward learning an end-to-end image processing pipeline. *IEEE Transactions on Image Processing*, 28(2):912–923, 2019. 3

[23] Yawar Siddiqui, Lorenzo Porzi, Samuel Rota Bulo´, Norman Mu¨ller, Matthias Nießner, Angela Dai, and Peter Kontschieder. Panoptic lifting for 3d scene understanding with neural fields, 2022. 2

[24] Pinzhuo Tian, Zhangkai Wu, Lei Qi, Lei Wang, Yinghuan Shi, and Yang Gao. Differentiable meta-learning model for few-shot semantic segmentation, 2019. 1, 2

[25] Ethan Tseng, Ali Mosleh, Fahim Mannan, Karl St.-Arnaud, and Felix Heide. Differentiable compound optics and processing pipeline for end-to-end raw image processing. In *ACM Transactions on Graphics (SIGGRAPH)*, 2021. 3

[26] Lijun Wang, Yifan Sun, Qiang Fu, and Wolfgang Heidrich. Differentiable optimization of freeform optics for vision tasks. *ACM Transactions on Graphics (TOG)*, 2022. 1, 2, 3

[27] Ruikang Xu, Chang Chen, Jingyang Peng, Cheng Li, Yibin Huang, Fenglong Song, Youliang Yan, and Zhiwei Xiong. Toward raw object detection: A new benchmark and a new model. In *2023 IEEE/CVF Conference on Computer Vision and Pattern Recognition (CVPR)*, pages 13384–13393, 2023. 2, 3

[28] Xinge Yang, Qiang Fu, and Wolfgang Heidrich. Curriculum learning for ab initio deep learned refractive optics. *Nature Communications*, 15(1):6572, 2024. 1, 2

[29] Fisher Yu, Haofeng Chen, Xin Wang, Wenqi Xian, Yingying Chen, Fangchen Liu, Vashisht Madhavan, and Trevor Darrell. BDD100K: A diverse driving dataset for heterogeneous multitask learning. In *Proceedings of the IEEE/CVF Conference on Computer Vision and Pattern Recognition (CVPR)*, pages 2636–2645, 2020. 5, 6

[30] Jingwei Zhang, Anh Tien Nguyen, Xi Han, Vincent Quoc-Huy Trinh, Hong Qin, Dimitris Samaras, and Mahdi S. Hosseini. 2dmamba: Efficient state space model for image representation with applications on giga-pixel whole slide image classification, 2025. 1, 2

[31] Xiangyu Zhang, Xinyu Zhou, Mengxiao Lin, and Jian Sun. ShuffleNet: An extremely efficient convolutional neural network for mobile devices. In *Proceedings of the IEEE/CVF Conference on Computer Vision and Pattern Recognition (CVPR)*, 2018. 2, 4

[32] Yichi Zhang, Xinge Yang, and Wolfgang Heidrich. Nanoscale differentiable optics design for computational imaging. *Nature Computational Science*, 2024. 1, 2, 3

[33] Hengshuang Zhao, Jianping Shi, Xiaojuan Qi, Xiaogang Wang, and Jiaya Jia. Pyramid scene parsing network, 2017. 5

[34] Runsong Zhu, Shi Qiu, Zhengzhe Liu, Ka-Hei Hui, Qianyi Wu, Pheng-Ann Heng, and Chi-Wing Fu. Rethinking end-to-end 2d to 3d scene segmentation in gaussian splatting, 2025. 2